

**Slow dynamics of a confined supercooled binary mixture. II.  $Q$  space analysis**

P. Gallo,\* R. Pellarin, and M. Rovere

*Dipartimento di Fisica, Università "Roma Tre," Istituto Nazionale per la Fisica della Materia, Unità di Ricerca Roma Tre and Democritos National Simulation Center, Via della Vasca, Navale 84, 00146 Roma, Italy*

(Received 25 September 2003; published 31 December 2003)

We report the analysis in the wave vector space of the density correlator of a Lennard-Jones binary mixture confined in a disordered matrix of soft spheres upon supercooling. In spite of the strong confining medium the behavior of the mixture is consistent with the mode-coupling theory predictions for bulk supercooled liquids. The relaxation times extracted from the fit of the density correlator to the stretched exponential function follow a unique power law behavior as a function of wave vector and temperature. The von Schweidler scaling properties are valid for an extended wave vector range around the peak of the structure factor. The parameters extracted in the present work are compared with the bulk values obtained in literature.

DOI: 10.1103/PhysRevE.68.061209

PACS number(s): 61.20.Ja, 61.25.-f

**I. INTRODUCTION**

Modifications of vitrification properties of liquids under confinement are of interest for relevant technological and biophysical problems [1,2]. While experiments show that the glass transition is not usually suppressed when the glass former is confined, changes in the temperature of the transition and in dynamical properties of liquids upon supercooling are induced by both the geometrical confinement and the interaction with the substrate [2].

In the study of the glass transition phenomenology the mode-coupling theory (MCT) of the evolution of glassy dynamics plays a fundamental role. MCT is able to describe the slowing down of supercooled liquids in a region of mild supercooling on approaching a temperature  $T_C$  [3–5]. This temperature marks a crossover from a region where dynamics is mastered by the transient caging of nearest neighbor to a lower temperature region where hopping processes dominate. In the ideal version of the theory, where hopping is not included, the nonlinear feedback mechanisms in the microscopic dynamics of the particles become so strong that they lead to the structural arrest of the system. Close to  $T_C$  MCT asymptotic solutions show analytic behaviors of the density correlator from which parameters of the theory can be extracted. These behaviors have been effectively found in experiments and simulations on supercooled liquids in regions close to  $T_C$  where hopping was negligible [5].

The role of the cooperative dynamics of the particles in the glass transition is still under discussion and there is an increasing activity on the definition and observation of dynamical heterogeneities [6]. Cooperativity in the dynamical behavior of the particles increases as the system is approaching the glass transition, suggesting the idea of the existence of a dynamic correlation length [7–11].

Molecular dynamics studies of model liquids in restricted geometries intended to assess the applicability of MCT can give an important contribution to the characterization of vitrification processes in confinement [12–16].

Liquids confined in network of interconnected pores with a large value of porosity, as silica xerogels, can be appropriately studied with models where the confining solid is built as a disordered array of frozen microspheres [17–19]. We consider here one such system. A liquid Lennard-Jones binary mixture (LJBM) composed of 80% of particles  $A$  and 20% of smaller particles  $B$  embedded in an off-lattice matrix of soft spheres. We performed molecular dynamics (MD) simulations of the confined LJBM upon supercooling in order to test the predictions of MCT.

The bulk phase of this LJBM behaves according to mode-coupling theory [20–22]. A preliminary analysis on our system [23] showed evidences that predictions of MCT hold also for the confined LJBM. A detailed study on the dynamics carried out in the direct space has shown two important differences with respect to the bulk upon supercooling [24]. The smaller  $B$  particles tend to avoid the soft sphere interfaces on lowering temperature and correspondingly their diffusion coefficient becomes lower than that of the  $A$  particles, at variance with the bulk where there is no such an inversion. Hopping processes are markedly present for both  $A$  and  $B$  particles already above  $T_C$  while in the bulk system only  $B$  particles show consistent hopping.

As a possible consequence of these differences, we observed that the range of validity of the power law fit to the diffusion coefficient as predicted by MCT in the long time region, late  $\alpha$ -relaxation region, appears much more limited than in the bulk.

A more refined assessment of the MCT validity can be obtained by a quantitative comparison between the asymptotic predictions of the theory and the results of our computer simulation in the  $(Q, t)$  space, where the density correlators of a liquid testing MCT display clear signatures of the approach to  $T_C$ . In this space important scaling relations of the theory can be verified. For these reasons we carry on here an analysis of the behavior of the self-intermediate scattering functions  $F_S(Q, t)$ .

In the following section we recall the predictions of the idealized version of MCT connected to our analysis. In Sec. III we describe our model system and molecular dynamics details. In Sec. IV we perform a test of MCT properties on our system. In particular, we analyze the static structure fac-

---

\*Author to whom correspondence should be addressed. Email address: gallop@fis.uniroma3.it

tor and the self-intermediate scattering function. For this latter quantity we perform numerical fit to MCT analytical laws and extract parameters of the theory. Last section is devoted to conclusions.

## II. MCT SCENARIO FOR THE EVOLUTION OF THE STRUCTURAL RELAXATION

The MCT for the evolution of glassy dynamics developed originally to deal with the cage effect provides a model for an ideal liquid-glass transition. The evolution of the structural relaxation is described in terms of the asymptotic behavior of density correlators near singularities which take place close to a crossover temperature  $T_C$ .

For a density correlator or any other correlator that couples with density fluctuations  $\phi(Q, t)$ , MCT predicts upon supercooling a diversification of relaxation times related to the nearest neighbor caging. In the short time regime the correlator show a fast relaxation associated with the ballistic motion of the particles. The high temperature correlator relaxes then exponentially for longer times. On lowering temperature for intermediate times a shoulder appears in the relaxation law. As the temperature is further lowered the shoulder enhances and becomes a plateau and the correlation function clearly shows a two step relaxation. The presence of the plateau is related to the trapping of the particle in the cage formed by its nearest neighbors. The time interval in which the correlation function is close to and above the plateau is called the  $\beta$ -relaxation region. The region that starts when the correlation function leaves the plateau is called the  $\alpha$ -relaxation region.

The long time limit of  $\phi(Q, t)$  is the nonergodicity parameter  $f_Q(T)$ . This parameter exhibits a singularity at a temperature  $T_C$  where the system undergoes an ideal transition from an ergodic to a nonergodic behavior.  $f_Q(T)$  jumps discontinuously from 0 above  $T_C$  to  $f_Q^c$  at  $T_C$ . On approaching  $T_C$  from below

$$f_Q - f_Q^c \sim \sqrt{|\epsilon|}, \quad (1)$$

where  $\epsilon = (T - T_C)/T_C$  is the small parameter of the theory and  $f_Q^c$  is called the critical nonergodicity parameter. On approaching  $T_C$  from above an effective  $f_Q$  can be identified with the height of the plateau of the correlator. In this range of temperatures the values of  $f_Q$  are very close to  $f_Q^c$  and show a very mild temperature dependence

$$f_Q - f_Q^c \sim O(\epsilon). \quad (2)$$

In the asymptotic limit where  $\epsilon \ll 1$  MCT predicts a factorization

$$\phi(Q, t) - f_Q^c = h_Q G(t). \quad (3)$$

where  $h_Q$  is a positive factor which does not depend on time. The so called  $\beta$  correlator  $G(t)$  obeys the scaling relation

$$G(t) \sim \sqrt{|\epsilon|} g(t/t_\epsilon), \quad (4)$$

where the time scale  $t_\epsilon$  has been introduced

$$t_\epsilon \sim \frac{t_0}{|\epsilon|^{1/2a}}. \quad (5)$$

Here  $t_0$  is a microscopic characteristic time of the system and the exponent  $a$  is called the critical exponent. In the time scale which corresponds to the decay of the correlator towards the plateau  $t \leq t_\epsilon$ ,

$$g(t/t_\epsilon) = (t_\epsilon/t)^a, \quad (6)$$

For the correlator decay of the liquid from the plateau

$$g(t/t_\epsilon) \sim (t/t_\epsilon)^b, \quad (7)$$

which is valid for times larger than the time scale of the  $\beta$  relaxation and much smaller than the  $\alpha$ -relaxation time  $\tau$ ,  $t_\epsilon \leq t \ll \tau$ . The exponent  $b$  is known as the von Schweidler exponent. The critical and the von Schweidler exponents are related by the formula

$$\lambda = \frac{[\Gamma(1-a)]^2}{\Gamma(1-2a)} = \frac{[\Gamma(1+b)]^2}{\Gamma(1+2b)}, \quad (8)$$

where  $\lambda$  is called the exponent parameter and  $\Gamma(x)$  is the Euler-Gamma function.

In the late part of the  $\alpha$ -relaxation regime the shape of the correlator of a liquid approaching the MCT crossover temperature [4] can be represented by means of the Kohlrausch-Williams-Watts (KWW) analytical function

$$\phi(Q, t) = f_Q \exp[-(t/\tau)^\beta], \quad (9)$$

where  $\beta$  is the Kohlrausch exponent.

The  $\alpha$ -relaxation time  $\tau$  is expected from MCT to follow the power law

$$\tau^{-1} \sim (T - T_C)^\gamma. \quad (10)$$

Both the exponent  $\gamma$  and the crossover temperature  $T_C$  should coincide with the ones appearing in the temperature dependence of the diffusion coefficient  $D \sim (T - T_C)^\gamma$ .

An important prediction of MCT is the validity of the time-temperature superposition principle. It states that in the low temperature regime, approaching from above the MCT crossover temperature, it is possible to time rescale the correlators evaluated at different  $T$  into a single master curve

$$\phi(t) = \tilde{\phi}(t/\tau(T)), \quad (11)$$

$\tilde{\phi}$  is the master function which in the late  $\alpha$ -relaxation limit becomes the KWW function (9).

In the late  $\beta$ , early  $\alpha$ -relaxation regime, Eq. (3), can be written as

$$\phi(Q, t) = f_Q^c - h_Q (t/\tau)^b. \quad (12)$$

This equation is called the von Schweidler law and  $\tau$  indicates a characteristic time of the system.

The exponent  $\gamma$  in Eq. (10) is related to the exponents  $a$  and  $b$  by the equation

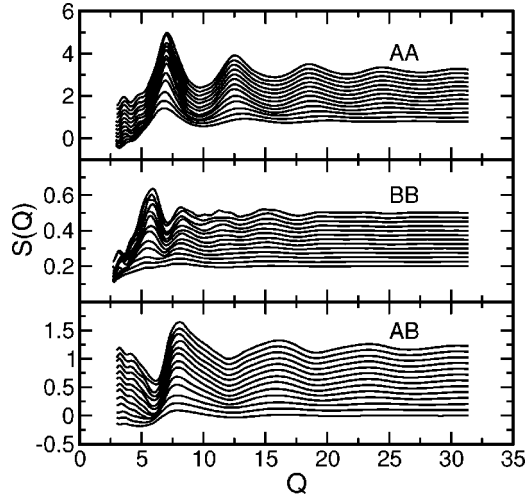


FIG. 1. Static structure factors. The temperatures corresponding to different curves are 5.0, 2.0, 0.8, 0.58, 0.538, 0.48, 0.465, 0.43, 0.41, 0.39, 0.37. For clarity we shifted up the lower temperature plots. For AA the shift is 0.2, for BB is 0.025, and for AB is 0.1.

$$\gamma = \frac{1}{2a} + \frac{1}{2b}. \quad (13)$$

While both  $\tau$  and the exponent  $\beta$  are  $Q$  dependent, the exponent  $b$  should not depend on  $Q$ . These two exponents are related:  $\beta > b$  and  $\beta(q \rightarrow \infty) = b$  [25].

### III. MODEL AND MOLECULAR DYNAMICS

The model studied consists of a rigid off-lattice matrix of 16 soft spheres where a liquid  $A_{80}B_{20}$  LJBM [21,22] is embedded. The mixture is composed of 1000 particles. In the following LJ units will be used. The parameters of the LJBM are  $\epsilon_{AA}=1$ ,  $\sigma_{AA}=1$ ,  $\epsilon_{BB}=0.5$ ,  $\sigma_{BB}=0.88$ ,  $\epsilon_{AB}=1.5$ , and  $\sigma_{AB}=0.8$ . The parameters of the soft sphere potential are  $\epsilon_{SA}=0.32$ ,  $\sigma_{SA}=3$ ,  $\epsilon_{SB}=0.22$ , and  $\sigma_{SB}=2.94$ . The box length is  $L=12.6$ . We performed molecular dynamics simulations in the NVE ensemble. We studied a set of temperatures ranging from  $T=5.0$  down to  $T=0.37$ . The time step for the lowest temperature is 0.02 and the largest production run consists in  $14 \times 10^6$  time steps. For all temperatures the time range investigated by MD was sufficient for the correlation functions to decay to zero in the long time limit. Further MD simulation details are reported in Refs. [23,24]. We did not find any qualitative differences in the behavior of the thermodynamic quantities with respect to the bulk upon supercooling [24].

### IV. ANALYSIS OF THE DYNAMICAL BEHAVIOR IN $(Q,t)$ SPACE

#### A. Static structure factor

In the framework of MCT the static structure factor is the input information for MCT equations [3,4]. This function is expected to depend smoothly on wave vectors and control parameters and it is also expected to show no singularities upon supercooling. In Fig. 1 we report the structure factors

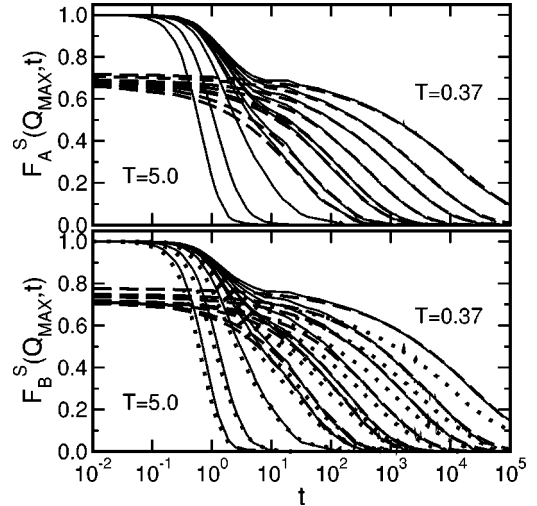


FIG. 2. Intermediate scattering function for A particles (upper panel) and for B particles (lower panel) for all the investigated temperatures. The continuous lines are calculated from the MD trajectories at the peaks of the structure factor  $Q_{MAX}^A=7.06$  and  $Q_{MAX}^B=5.90$ . The long dashed lines are the fit to the KWW stretched exponential function, see Eq. (9). In the lower graph the dotted lines are the A particles data, reported for comparison.

$S(Q)$  of the confined mixture for the temperatures investigated. They behave consistently with MCT as the functions smoothly vary upon supercooling implying no divergence of correlation length. No signature of phase separation of the mixture are evident in confinement as we already deduced from the analysis of the  $g_{AB}(r)$  [24]. We observe that there are no relevant discrepancies in the confined  $S_{ij}(Q)$  with respect to the bulk [22] neither in the shape nor in the peak positions. For  $Q$  values around the first structure factor peak MCT features are best evident in the density correlators. The peak positions in our confined LJBM show a very mild temperature dependence, especially for low temperatures. We will therefore consider them constant. The values  $Q_{MAX}^A=7.06$ ,  $Q_{MAX}^B=5.90$  will be used to test MCT as a function of temperature in the following. In the case of the bulk the values used were  $Q_{MAX}^{AA}=7.25$  and  $Q_{MAX}^{BB}=5.75$ , respectively.

#### B. Self-intermediate scattering function

We consider now the self-intermediate scattering function (SISF) defined as

$$F_S(Q,t) = \frac{1}{N} \left\langle \sum_i e^{-i\vec{Q} \cdot \vec{R}_i(0)} e^{i\vec{Q} \cdot \vec{R}_i(t)} \right\rangle. \quad (14)$$

This correlator can be used to test the predictions of MCT close to  $T_C$  as described in Sec. II. In Fig. 2 the SISF of our confined system is plotted for all considered temperatures and for both particle types at the peak of the structure factors. At high temperatures the correlators relax exponentially for longer times. On lowering temperature we observe the onset of the plateau related to the two step relaxation typical of a supercooled liquid.

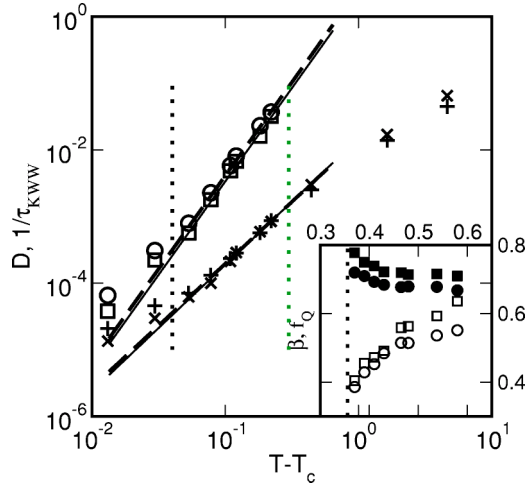


FIG. 3. In the main frame, values of the relaxation time  $\tau$  obtained from the fit to the KWW of the SISF (see Fig. 2) for  $A$  (empty circles) and  $B$  (empty squares) particles. In the same graph values of the diffusion coefficients  $D$  obtained from the MSD [24] for  $A$  (+) and  $B$  ( $\times$ ) particles. The power law fits are also plotted. These fits are performed on the temperature window  $0.41 \leq T \leq 0.58$ , limited by vertical dotted lines. Dashed lines are the fit for  $A$  and continuous lines are the fit for  $B$  particles. Parameters obtained from the fit are reported in Table I. In the inset  $f_Q$  for  $A$  (filled circles) and  $B$  (filled squares) particles and stretching exponent  $\beta$  for  $A$  (empty circles) and  $B$  (empty squares) particles are reported.

An onset temperature for the plateau of  $T \approx 0.6$  can be identified for our system. The corresponding temperature for the bulk is  $T \approx 1.0$ . Analogous to bulk supercooled liquids for the lowest temperature we observe that correlators stretch several decades in time. We also see that  $A$  and  $B$  particles relax in a similar fashion but larger  $A$  particles relax faster at this wave vector, especially for lower temperatures. This counterintuitive phenomenon that happens only in confinement is possibly connected to packing constraints. We have in fact detected that on lowering temperature smaller  $B$  particles tend to avoid the soft sphere interfaces and preferentially move in the center of the interstices. Correspondingly diffusion coefficients of  $A$  and  $B$  particles extracted from the mean square displacement (MSD) show an inversion as supercooling progresses [24].

### C. Kohlrausch-Williams-Watts analysis of the self-intermediate scattering function

In Fig. 2 together with the SISF we show the fit to the KWW function, as defined in Eq. (9), performed for temperatures  $T < 0.8$  in the  $\alpha$ -relaxation region for both  $A$  and  $B$  particles. A remarkable agreement with the data is found. From the fit the KWW relaxation time  $\tau$ , the stretching exponent  $\beta$ , and the effective nonergodicity parameter  $f_Q$  are extracted.

MCT predicts both  $D$  and  $\tau^{-1}$  to follow the same power law, see Eq. (10). The relaxation times  $\tau$  are shown in the mainframe of Fig. 3. In the same picture we show the diffusion coefficients  $D$  previously reported and obtained from

TABLE I. Values of the parameters of Eq. (10) extracted from the fit to  $\tau$  and  $D$ . Values for the bulk system are from Refs. [21,22].

	$T_C^A$	$T_C^B$	$\gamma^A$	$\gamma^B$
Confined system				
From $\tau$	0.355	0.355	2.90	2.89
From $D$	0.356	0.356	1.86	1.89
Bulk system				
From $\tau$	0.432	0.432	2.6	2.6
From $D$	0.435	0.435	2.0	1.7

the slope of the MSD [24]. We also display in the figure the fit to the MCT predicted behavior. Values of  $T_C$  and  $\gamma$  obtained from the fit are reported in Table I. We observe that both in bulk and confined system the crossover temperature  $T_C$  extracted from  $D$  and  $\tau$  and from  $A$  and  $B$  particles coincide. A substantial reduction of  $T_C$  is observed in confinement,  $T_C \approx 0.36$ . The bulk value reported in literature is  $T_C \approx 0.43$ .

The exponents  $\gamma$  which determine the slope of the fit are the same for  $A$  and  $B$  particles both for  $\tau$  and  $D$ . This agrees with the prediction of MCT that these exponents should be universal and do not depend on the species of the particles involved. A discrepancy with respect to MCT prediction is represented by the different value of  $\gamma$  between  $D$  and  $\tau$ . As we can see from the table the same discrepancy affects the mixture also in the bulk phase and it may be due to long time activated processes causing a breakdown of the predictions of the theory only for quantities calculated at extremely long times [24]. In fact in confinement, where hopping is consistent for both  $A$  and  $B$  particles, a reduction of circa 35% is observed for  $\gamma$  in going from  $\tau$  to  $D$ . In the bulk phase, where hopping is more consistent for  $B$  particles, the reduction observed is 30% for  $B$  and 20% for  $A$  particles.

A substantial shrinkage of the range of validity of the theory is found in confinement. In Fig. 3, we in fact see that the MCT predicted power law behavior is verified for  $\tau$  in the temperature window  $0.58 \leq T \leq 0.41$ , the same found for the  $D$  coefficients [24], which corresponds to  $0.153 < \epsilon < 0.631$  while in the bulk  $0.07 < \epsilon < 1.30$  [20].

The values of the parameters  $f_Q$  and  $\beta$  extracted from the fit are plotted as a function of temperature in the inset of Fig. 3. We note that the effective nonergodicity parameter  $f_Q$  only slightly depends on temperature in agreement with MCT that predicts a consistent temperature dependence of this factor only below  $T_C$ . The stretching parameter  $\beta$  decreases upon lowering the temperature as also expected, but we observe no flattening of this exponent on approaching  $T_C$  as found for bulk systems. Besides, correlators appear much more stretched in confinement. In the bulk  $\beta > 0.78$  while here the lowest values are slightly below 0.4.

We report in Fig. 4 the temporal evolution of the correlators for different wave vectors  $Q$  ranging from 2.5 to 14.5 for the temperature  $T = 0.41$ . In the same picture we also show the fit to the KWW function. A remarkable agreement is found. The height of the plateau strongly depends on  $Q$ . The

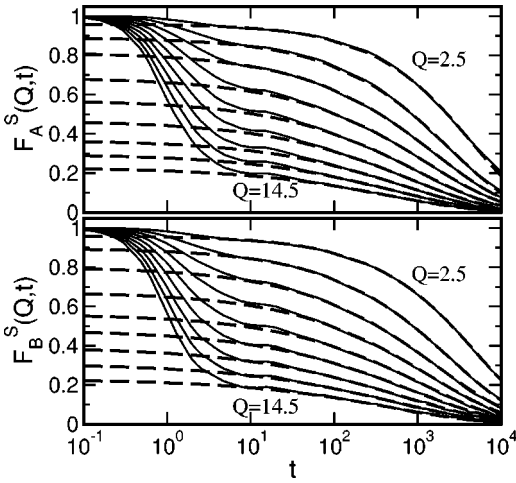


FIG. 4. Wave vectors analysis at  $T=0.41$ . The range for both particles is  $2.5 \leq Q \leq 14.5$ , with a step of  $\delta Q = 1.5$ . The KWW fit (long dashed lines) is also shown.

same analysis was performed for  $T = 0.58, 0.48, 0.43, 0.39$  (not shown).

The values of the parameters of the fit are reported for all the above temperatures in Fig. 5. All the parameters show a monotonic behavior in  $Q$ . In particular, at high temperature the relaxation time  $\tau$  spans two decades. It is worth noting that the  $\beta$  exponent is converging for  $T \rightarrow T_C$  and for  $Q \rightarrow \infty$  to the value of  $b$  for both types of particles as expected [25]. Finally we note that the prefactor  $f_Q$  is slightly  $T$  dependent for all  $Q$ .

In Fig. 6 the  $\tau$  values extracted from the fit are reported as a function of the shifted temperature  $T - T_C$ . In the temperature range where the power law behavior is effective, that for

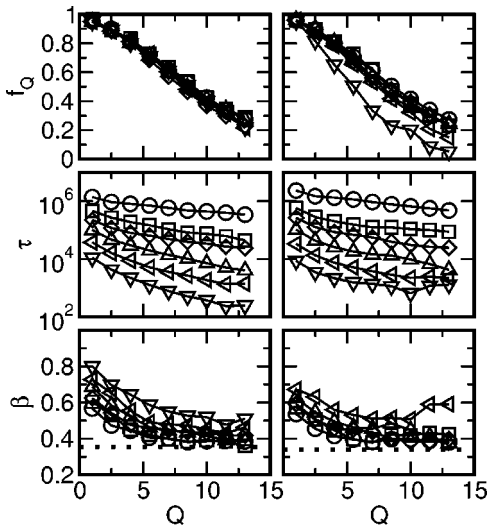


FIG. 5. In the graphs are shown the KWW parameters  $f_Q$ ,  $\tau$ ,  $\beta$  upon varying the wave vector  $Q$ , for  $A$  (panels on the left) and  $B$  particles (panels on the right). The various symbols refer to different temperatures: circle 0.37, square 0.39, diamond 0.41, triangle up 0.43, triangle left 0.48, triangle down 0.58. The dotted line of the bottom panels refers to the values extracted from the von Schweidler fit  $b_A = 0.355$  and  $b_B = 0.350$ .

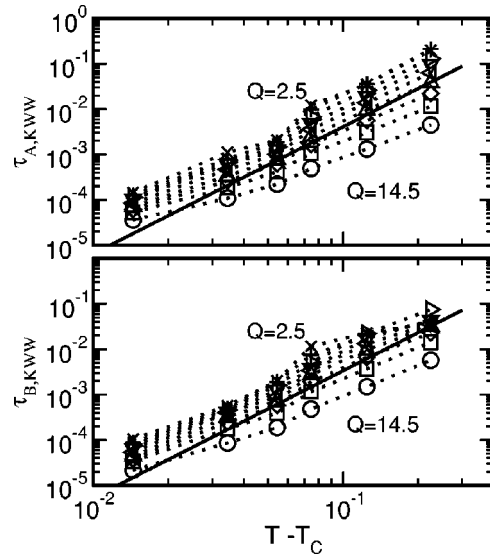


FIG. 6. Relaxation times  $\tau$  (symbols) vs shifted temperature  $T - T_C$ . Various symbols represent different  $Q$ . The slope of the overlaid straight line corresponds to  $\gamma = 2.9$ .

our system is  $0.41 \leq T \leq 0.58$ ,  $\gamma$  is expected to be independent on  $Q$ . In Fig. 6 we effectively observe that the curves are parallel to each other and parallel to the straight line overlaid that corresponds to the value of  $\gamma = 2.9$  extracted from the fit performed at the peak of the structure factor (see Table I).

**D. von Schweidler test for the self-intermediate scattering function**

According to Eq. (11) the time dependence of the correlation functions can be rescaled by the relaxation time  $\tau$  extracted from the fit to the KWW. The curves for the lowest temperatures are expected to collapse onto a mastercurve in

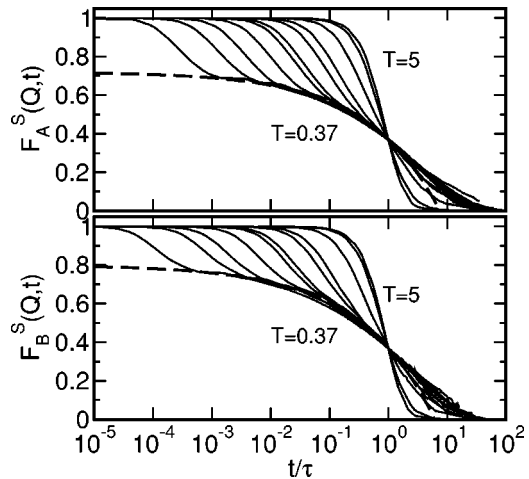


FIG. 7. Intermediate scattering functions of Fig. 2 rescaled with respect to the corresponding KWW relaxation time for both  $A$  (top panel) and  $B$  (bottom panel) particles. The dashed curves represent the von Schweidler fit.

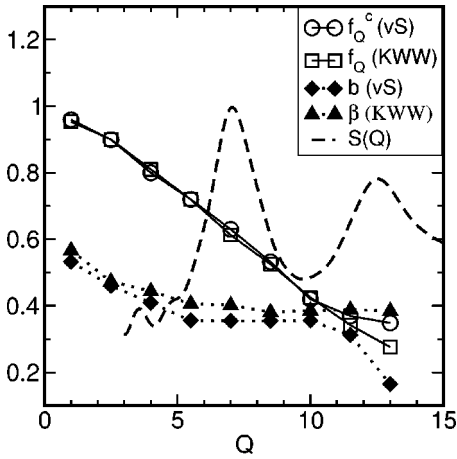


FIG. 8. Values of the parameters of the von Schweidler fit (black diamond, white circles) and for comparison the parameters of the KWW (black triangles, white squares) upon varying  $Q$  for  $A$  particles. The static structure factor is represented by the dotted line at  $T=0.37$ .

the late  $\beta$ -, early  $\alpha$ -relaxation region. In Fig. 7 we report for both particle types the master plot of the SISF of Fig. 2. In the same figure we show the fit to the von Schweidler functional form of Eq. (12).

The values of the parameters obtained for  $A$  and  $B$  particles from the fit are

$$f_{Q,A}^c = 0.72, \quad h_{Q,A} = 0.35, \quad b_A = 0.355;$$

$$f_{Q,B}^c = 0.79, \quad h_{Q,B} = 0.44, \quad b_B = 0.350.$$

In the bulk the values of the exponent  $b$  are 0.51 for  $A$  and 0.46 for  $B$  particles, respectively while we observe that in confinement  $b$  values are lower and almost the same. This might indicate that hopping is influencing also the earlier  $\alpha$ -relaxation region.

An important prediction of MCT is that the von Schweidler  $b$  value should be independent of the wave vector  $Q$ . This test was performed in the bulk [22], where the authors stressed a small dependence of  $b$  between  $Q_{MAX}$  and  $Q_{MIN}$ , where  $Q_{MIN}$  is the position of the first minimum after the peak of the static structure factor. In Fig. 8 the values for  $f_Q^c$  and  $b$  are presented as a function of  $Q$  for  $A$  particles. The values for  $f_Q$  and  $\beta$  for the KWW and the  $S(Q)$  are also shown. The  $f_Q$  factors are in perfect agreement with the Gaussian behavior predicted by the MCT and found in the bulk simulations. We can therefore consider the  $f_Q$  KWW factors as a good approximation of the critical nonergodicity parameter  $f_Q^c$  at such low temperature. The  $b$  parameter decreases monotonically, except between the first  $S(Q)$  maximum and the following minimum where it is practically constant, similar to the bulk. We note that the  $\beta$  values are always higher than the relative  $b$  values, this is a consequence of the fact that the KWW can describe the late  $\alpha$  but not the late  $\beta$ , early  $\alpha$  regime where the data are well fitted by the von Schweidler law.

In our correlators oscillations, possibly due to finite size effects, in the time zone where the power law of Eq. (6)

holds, prevents us from calculating the exponent  $a$  of MCT directly. It is still possible to evaluate the parameter  $a$  from the closure relation of Eq. (13). Using the  $\gamma$  calculated from  $\tau$  and the von Schweidler exponent  $b$  found previously, the values of the critical exponent  $a$  for the two species are, respectively,

$$a_A = 0.335, \quad a_B = 0.342.$$

These values are quite high, although within the topmost value indicated by the theory  $a \leq 0.395$ .

## V. SUMMARY AND CONCLUSIONS

We have studied the dynamics of a model glass former in confinement. This study is intended to assess the validity of MCT for supercooled liquids embedded in strongly repulsive and highly confining environments. Our model consists in a LJBM embedded in a disordered matrix of soft spheres. It represents a possible modelization for liquids hosted in silica xerogels.

The analysis performed in  $r$  space and previously reported [24] showed that the MSD behavior can be interpreted for both  $A$  and  $B$  particles in terms of the onset of the cage effect and that the diffusion coefficients  $D$  extracted from the MSD can be fitted with the power law predicted by MCT. There is however a clear evidence that the range of validity of the MCT predictions in the late  $\alpha$ -relaxation region suffers a reduction of 60% with respect to the bulk. In terms of the small parameter of the theory  $\epsilon$  the bulk range is  $0.07 < \epsilon < 1.30$ , while in the confined system it results to be  $0.153 < \epsilon < 0.631$ . We inferred that the upper bound reduction might be due to the fact that  $B$  particles tend to avoid the soft sphere interfaces in lowering temperature. The MCT power law starts in fact to hold for  $D$  only when most  $B$  particles are avoiding the soft spheres [24]. The lower bound reduction is to be connected to the presence of important hopping processes more marked with respect to the bulk, which tend to introduce deviations from the ideal MCT predictions earlier than in bulk.

We have presented here an analysis in  $(Q, t)$  space of the confined LJBM by considering the SISF and we have tested the main scaling relations of MCT.

The static structure factor is similar to that of the bulk phase. The SISF is well fitted with the stretched exponential function and the power law behavior of the  $\alpha$ -relaxation times  $\tau$  extracted for both  $A$  and  $B$  particles is consistent with MCT. Power law fit to both  $D$  and  $\tau$  as a function of temperature give the same value for the crossover temperature  $T_C = 0.355$ . We observe a reduction of circa 20% of  $T_C$  in going from bulk to confined which can be ascribed to the existence of an upper bound in confinement for the size of the domains of cooperative dynamics. A discrepancy observed in the values of the exponents  $\gamma$  obtained for  $D$  and  $\tau$  is to be connected to the more important presence of hopping processes in confinement. Hopping processes influence in fact the behavior of  $D$  more than that of  $\tau$  causing a decrease of the value of the exponent. This discrepancy was present also in the bulk.

The existence of a confining disordered host structure seems to be connected also to the lowering of the stretching parameter possibly caused by a larger distribution of relaxation times with respect to the bulk.

The behavior of the SISF as a function of  $Q$  is very similar to that of the bulk. All parameters show a monotonic behavior as a function of  $Q$  and the stretching exponent approaches  $b$  for high  $Q$ . The exponent  $\gamma$  shows no  $Q$  dependence.

The SISF plotted against  $t/\tau$  shows a scaling behavior. The mastercurve can be fitted with the von Schweidler function in the late  $\beta$ , early  $\alpha$  region. Analogous to the bulk, the exponent  $b$  is practically constant between the first maximum and the following minimum of the structure factor. Similar to  $\beta$  a substantial reduction of  $b$  is observed in going from bulk to confined LJBM.

The exponent parameter  $\lambda$  of the system can be calculated from Eq. (8). Contrary to MCT prediction we get different values of  $\lambda$  on using the exponent  $a$  or the exponent  $b$  in Eq. (8)

$$\lambda_{a,A}=0.680, \quad \lambda_{b,A}=0.871;$$

$$\lambda_{a,B}=0.663, \quad \lambda_{b,B}=0.873.$$

This inconsistency is present also in the bulk but it is much less severe. The value of  $\lambda$  reported for the bulk is  $0.79 \pm 0.04$ . Here we have a much larger uncertainty that leads to  $0.8 \pm 0.1$ .

Considering the strong confinement experienced by the LJBM, the agreement between MCT predictions and the behavior of our confined system as a function of  $T$  and  $Q$  is most remarkable. Differences in behavior with respect to the bulk on approaching  $T_C$  are in fact to be ascribed to the presence of more relevant hopping effects.

The possibility to connect the decrease of  $T_C$  and the enhancement of hopping effects in confinement with a key role played by dynamical heterogeneities in the glass transition scenario is an issue that would deserve to be addressed in future studies.

- 
- [1] For a review on metastable liquids see, P. G. Debenedetti, *Metastable Liquids: Concepts and Principles* (Princeton University Press, Princeton, 1997).
- [2] See, for example, in *Proceedings of the International Workshop on Dynamics in Confinement*, edited by B. Frick, R. Zorn, and H. Büttner [J. Phys. IV **10** (Pr7), 1–347 (2000)]; Eur. Phys. J. E **12** (2003).
- [3] W. Götze and L. Sjögren, Rep. Prog. Phys. **55**, 241 (1992).
- [4] W. Götze, in *Liquids, Freezing and Glass Transition*, edited by J. P. Hansen, D. Levesque, and J. Zinn-Justin (North Holland, Amsterdam, 1991).
- [5] W. Götze, J. Phys.: Condens. Matter **11**, A1 (1999).
- [6] G. Adam and J. Gibbs, J. Chem. Phys. **43**, 139 (1965).
- [7] C. Donati, J.F. Douglas, W. Kob, S.J. Plimpton, P.H. Poole, and S.C. Glotzer, Phys. Rev. Lett. **80**, 2338 (1998).
- [8] C. Donati, S.C. Glotzer, and P.H. Poole, Phys. Rev. Lett. **82**, 5064 (1999).
- [9] B. Doliwa and A. Heuer, Phys. Rev. Lett. **80**, 4915 (1998).
- [10] B. Doliwa and A. Heuer, Phys. Rev. E **61**, 6898 (2000).
- [11] L. Berthier, Phys. Rev. Lett. **91**, 055701 (2003).
- [12] P. Gallo, E. Spohr, and M. Rovere, Phys. Rev. Lett. **85**, 4317 (2000).
- [13] P. Gallo, E. Spohr, and M. Rovere, J. Chem. Phys. **113**, 11 324 (2000).
- [14] F. Varnik, J. Baschnagel, and K. Binder, Phys. Rev. E **65**, 021507 (2002).
- [15] P. Scheidler, W. Kob, and K. Binder, Europhys. Lett. **52**, 277 (2000).
- [16] P. Scheidler, W. Kob, and K. Binder, e-print cond-mat/0309025.
- [17] M. L. Rosinberg, in *New Approaches to Problems in Liquid State Theory*, edited by C. Caccamo, J. P. Hansen, and G. Stell (Kluwer Academic, Dordrecht, MA, 1999).
- [18] L. Sarkisov and P.A. Monson, Phys. Rev. E **61**, 7231 (2000).
- [19] K.S. Page and P.A. Monson, Phys. Rev. E **54**, R29 (1996).
- [20] W. Kob and H.C. Andersen, Phys. Rev. Lett. **73**, 1376 (1994).
- [21] W. Kob and H.C. Andersen, Phys. Rev. E **51**, 4626 (1995).
- [22] W. Kob and H.C. Andersen, Phys. Rev. E **52**, 4134 (1995).
- [23] P. Gallo, R. Pellarin, and M. Rovere, Europhys. Lett. **57**, 212 (2002).
- [24] P. Gallo, R. Pellarin, and M. Rovere, Phys. Rev. E **67**, 041202 (2003).
- [25] M. Fuchs, J. Non-Cryst. Solids **172-174**, 241 (1994).